Available online at www.sciencedirect.com
SCIENCE DIRECT
Journal of Catalysis 232 (2005) 467–475
JOURNAL OF CATALYSIS
www.elsevier.com/locate/jcat

A kinetic study of vinyl acetate synthesis over Pd-based catalysts: kinetics of vinyl acetate synthesis over Pd–Au/SiO_2 and Pd/SiO_2 catalysts

Y.-F. Han [1], J.-H. Wang, D. Kumar, Z. Yan, D.W. Goodman *

Department of Chemistry, Texas A&M University, College Station, TX 77843-3255, USA

Received 11 January 2005; revised 22 March 2005; accepted 4 April 2005

Available online 10 May 2005

Abstract

Kinetic studies of vinyl acetate (VA) synthesis were carried out for Pd (1.0 wt%)/SiO_2 and Pd (1.0 wt%)–Au (0.5 wt%)/SiO_2 catalysts, with highly dispersed metal particles (Pd and Pd–Au) characterized by X-ray diffraction and transmission electron microscopy–energy dispersive spectroscopy (TEM-EDS). The kinetics of the related CO oxidation reaction were also explored. The kinetics of VA synthesis and CO oxidation reactions proceed via a Langmuir–Hinshelwood mechanism. For Pd-only catalysts, dissociative adsorption of O_2 is believed to be the rate-determining step. This step is suppressed by adsorbed CO/C_2H_4 and gives rise to a negative reaction order with respect to CO/C_2H_4 and a positive order with respect to O_2. However, the reaction mechanism was significantly modified by the addition of Au to Pd, as indicated by the change in the reaction order with respect to CO/C_2H_4; in particular, the order with respect to C_2H_4 becomes positive. The modification of the mechanism for the Pd–Au catalyst correlates with the reduction in the concentration of Pd–Pd ensembles upon alloying with Au. By TEM-EDS, Au surface enrichment was detected for the Pd–Au alloy, and the interaction between Au and Pd leads to a formation of more active Pd ensembles, such as $PdAu_5$ and $PdAu_6$. The surface properties of Pd versus Pd–Au catalysts were explored by CO/C_2D_4-TPD on thick films of Pd and Pd–Au. These studies indicate that the adsorption sites on Pd are significantly modified by Au; concurrently, the bonding of CO and C_2D_4 to Pd in the Pd–Au alloy also varied. As a result, the coverage of CO and C_2H_4 on the Pd–Au surface decreased markedly. The enhanced capacity of the Pd–Au surface for oxygen and/or the enhanced mobility of adsorbed oxygen under the reaction conditions are likely responsible for the unusually high reactivity of Pd–Au alloy catalysts for VA synthesis.

Keywords: Vinyl acetate synthesis; CO oxidation; XRD; TEM-EDS; CO-TPD; C_2D_4-TPD; Kinetics; Catalysis; Pd/SiO_2; Pd–Au/SiO_2; Pd film; Pd–Au film

1. Introduction

The synthesis of vinyl acetate (VA) from ethylene (C_2H_4), acetic acid (AcOH), and oxygen (O_2) is an important industrial reaction [1–4]. The ideal reaction pathway is

$$C_2H_4 + CH_3COOH + \frac{1}{2}O_2 \rightarrow C_2H_3OOCCH_3 + H_2O. \quad (1)$$

It is well known that the performance of a Pd–Au alloy catalyst for this reaction is superior to a Pd-only catalyst [2,5–9]. Theoretical studies [10,11] suggest that VA synthesis over Pd requires rather large ensembles and is a structure-sensitive reaction. It is plausible that the electronic and geometric properties of Pd particles can be tuned by formation of a Au_xPd_y alloy surface with highly optimized sites for VA synthesis [12–19].

The modification of the electronic and geometric properties of Pd upon alloying with Au has been extensively studied because of the enhanced properties of Pd–Au catalysts for several reactions including VA synthesis [10–19]. However, how the structure of the Pd–Au surface is altered

* Corresponding author.
E-mail address: goodman@mail.chem.tamu.edu (D.W. Goodman).
[1] Present address: Institute of Chemical and Engineering Sciences, Singapore 627833.

0021-9517/$ – see front matter
doi:10.1016/j.jcat.2005.04.001

upon alloying and how this modification affects the catalytic properties are unclear, especially with respect to the adsorption of the reactants, such as ethylene, acetic acid, and oxygen. Temperature-programmed desorption (TPD) is an effective method for addressing questions related to the surface composition of the Pd–Au alloy surface. Therefore ethylene (C_2D_4) and CO TPD studies were carried out on multilayer films of Pd and Pd–Au prepared on a single-crystal Mo(110) surface.

A rather complete picture of CO adsorption and oxidation on Pd surfaces has been developed in UHV [20–24] and under realistic reaction conditions [25,26]. In particular, according to studies on single crystals of Pd(100), Pd(110), and Pd(111) [27], CO oxidation on a Pd surface exhibits a subtle structure sensitivity similar to that observed for VA synthesis. Therefore, parallel studies of the kinetics of CO oxidation, including the adsorption of CO on catalysts used for VA synthesis, were undertaken to aid our understanding of the VA reaction mechanism on Pd-based catalysts.

Previously we reported on the kinetics of VA synthesis [9] and ethylene combustion [28] (primarily a side reaction in VA synthesis) over Pd/SiO_2 catalysts with varying Pd particle sizes and proposed that the dissociative adsorption of O_2 on Pd-only catalysts is rate-limiting. However, a detailed kinetics study of VA synthesis on silica-supported Pd–Au alloy catalysts has not been undertaken. Furthermore, a comparison of the kinetics of VA synthesis over Pd-only and Pd–Au alloy catalysts should be helpful in detailing the mechanism of VA synthesis. In particular, in this study the structural modification of the Pd surface upon alloying with Au and how alloying influences the mechanisms of VA synthesis and CO oxidation are addressed. Parallel TPD studies of CO and C_2D_4 adsorption/desorption have also been carried out.

2. Experimental

2.1. Catalyst preparation and kinetics measurements

The Pd (1.0 wt%)/SiO_2 and Pd (1.0 wt%)–Au (0.5 wt%)/SiO_2 (atomic ratio of Pd/Au $\approx$ 4:1) catalysts, designated as Pd-only and Pd–Au, respectively, were prepared by the incipient wetness method; their preparation has been described in detail elsewhere [2,9]. A high-surface-area SiO_2 (Aldrich; no. 7631-86-9, 600 m^2/g, particle size 230–400 mesh, pore volume of 1.1 ml/g) was used as the support. The catalytic activity was measured with a micro fixed-bed reactor connected to an online GC. The methodologies for measuring the VA synthesis kinetics and calculation of the kinetic parameters have been described in detail [28]. In addition, CO oxidation was carried out in the same system by variation of the partial pressure of CO and O_2 between 3.0 and 10.0 kPa. The conversion of CO was maintained at $< 10\%$; the reaction rates are expressed with respect to the CO_2 produced.

2.2. Characterization of the supported Pd and Pd–Au catalysts

2.2.1. Transmission electron microscopy–energy dispersive spectroscopy (TEM-EDS)

The samples were ultrasonically dispersed in an ethanol solvent and then dried over a carbon grid. The metal particles were imaged with a JOEL 2010 microscope; at least 200–300 particles were measured to obtain the average particle size distributions. The surface composition of specific areas and individual Pd–Au particles were analyzed by energy-dispersive X-ray analysis (EDS) with the use of the Au L (9.710 keV) and Pd L (2.839 keV) lines.

2.2.2. X-ray-diffraction (XRD)

X-ray powdered diffraction data were obtained with a Bruker D8 diffractometer and Cu-K_α radiation. The samples were scanned over a Bragg angle (2θ) range of 36°–50°.

2.3. CO/C_2D_4-TPD on Pd and Pd–Au films

The experiments were carried out in a conventional UHV chamber coupled to an in situ elevated pressure IR cell. The UHV chamber (base pressure of $< 1 \times 10^{-10}$ Torr) was equipped with an Auger electron spectrometer (AES) and a quadrupole mass spectrometer (QMS). The Mo(110) single crystal was mounted on a translatable probe that could be cooled to 80 K by liquid N_2 and heated to 1500 K by resistive heating or to 2000 K by electron beam heating. The sample temperature was measured with a type C thermocouple spot-welded to the edge of the crystal.

The TPD experimental procedure was as follows. First, Pd (10 ML) was deposited on a Mo(110) surface at room temperature, and the cleanliness and coverage established by AES. Next, the sample was cooled to 80 K and CO or C_2D_4 adsorbed. We prepared Pd–Au films by first depositing Pd then Au in a 1:1 Pd/Au atomic ratio. CO (99.995% purity; Matheson) and C_2D_4 (isotopic content 99%; Aldrich) were stored in glass bulbs and used without further purification. A detailed description of the TPD methodology is published elsewhere [29].

3. Results

3.1. Characterization of the high-surface-area Pd/SiO_2 and $Pd–Au/SiO_2$ catalysts

For comparison, XRD patterns (obtained before reaction) of the Pd-only and Pd–Au catalysts, which we prepared by heating the catalyst precursor in a mixture of O_2/N_2 at 673 K for 30 min followed by reduction in pure H_2 at 573 K for 30 min, are shown in Fig. 1. The feature at $2\theta = 40.1°$ for the Pd-only catalyst in Fig. 1A, corresponding to Pd(111) in a Pd crystallite, shifts to 39.7° for the Pd–Au catalyst in Fig. 1B,

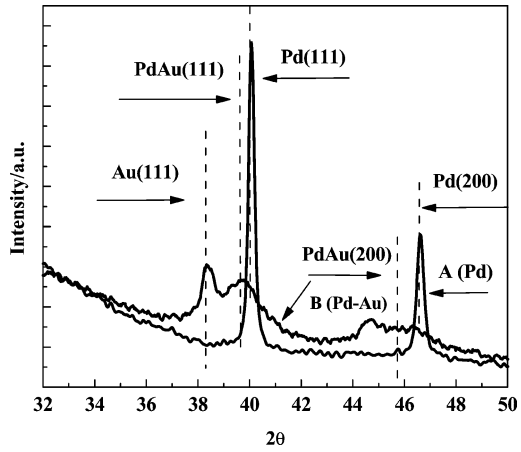

Fig. 1. XRD patterns for an unreacted Pd-only (A) and Pd–Au (B) catalysts pretreated as follows: in O_2 (10%)/N_2 at 673 K for 30 min with a flow rate of 20 ml/min, followed by a reduction in H_2 at 573 K for 30 min with the same flow rate.

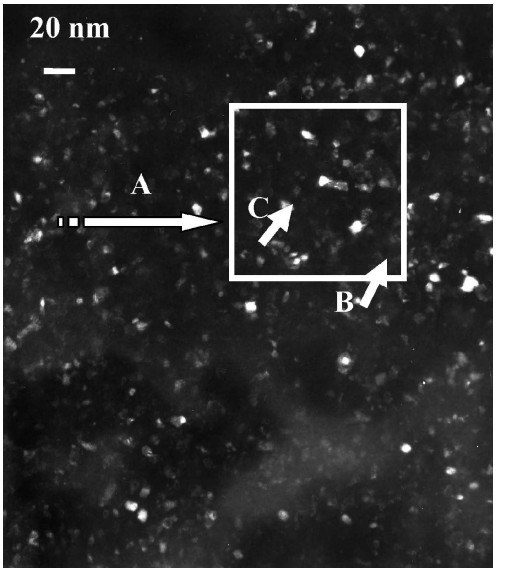

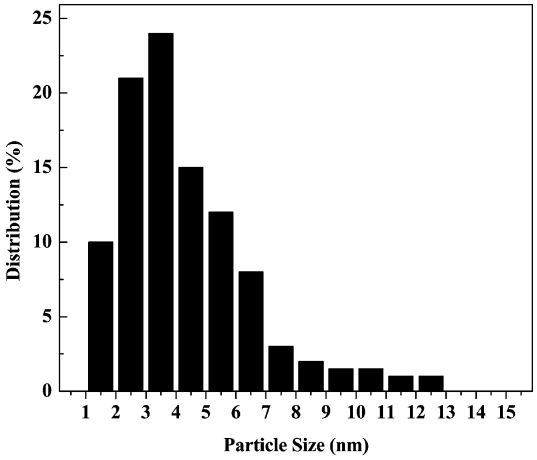

Fig. 2. TEM image of Pd–Au clusters for the unreacted Pd–Au catalyst (top, same as Fig. 1), atomic ratio of Pd/Au in region A = 2/1, at particle B = 2.2/1 and C = 1.9/1; the Pd–Au cluster distribution is shown at the bottom.

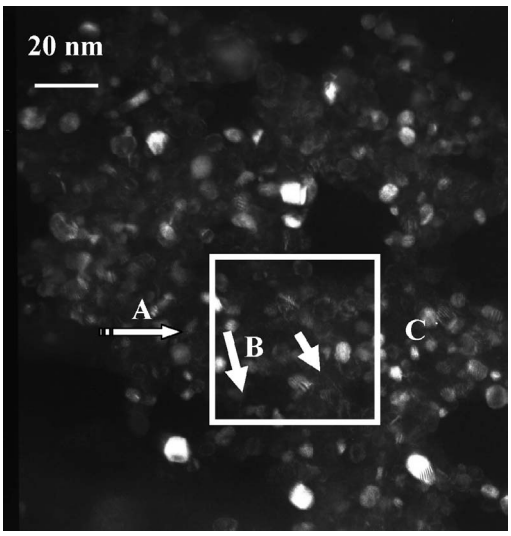

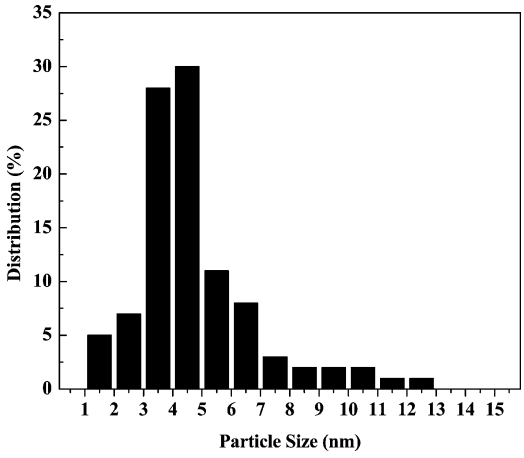

Fig. 3. TEM image of Pd–Au clusters for the reacted Pd–Au catalyst (top, for VA synthesis in a mixture of C_2H_4 = 7.5 kPa, O_2 = 1.0 kPa, AcOH = 2.0 kPa, remainder N_2, at 413 K for 100 h), atomic ratio of Pd/Au in region A = 1.5/1, at particle B = 1.1/1 and C = 1.3/1; the Pd–Au cluster distribution is shown at the bottom.

which is indicative of the formation of a Pd–Au(111) alloy phase.

The TEM results of Figs. 2 and 3 show that the sizes of the Pd–Au particles are distributed broadly over the range of 1.0–13.0 nm, and most of the particle diameters lie between 2.0 and 5.0 nm. The corresponding average diameter is 3.2 nm for the Pd–Au before reaction (Fig. 2) and 4.2 nm after reaction (Fig. 3). Surface composition determined by EDS indicates that the average Pd/Au atom ratio in region A in Fig. 2 (top) is 2.0, lower than the initially deposited ratio of 4.0; ratios of 2.2 and 1.9 were observed for particles B and C, respectively. However, the ratio of Pd/Au decreased to 1.5 after reaction, as shown in region A of Fig. 3 (top), whereas the ratios for particles B and C in region A are 1.1 and 1.3, respectively. For the Pd-only catalyst, the average diameter of Pd particles in the reduced catalyst is ca. 2.5 nm, which increased to 3.5 nm after reaction. The TEM images and Pd particle distributions for the Pd-only catalyst have been reported elsewhere [9].

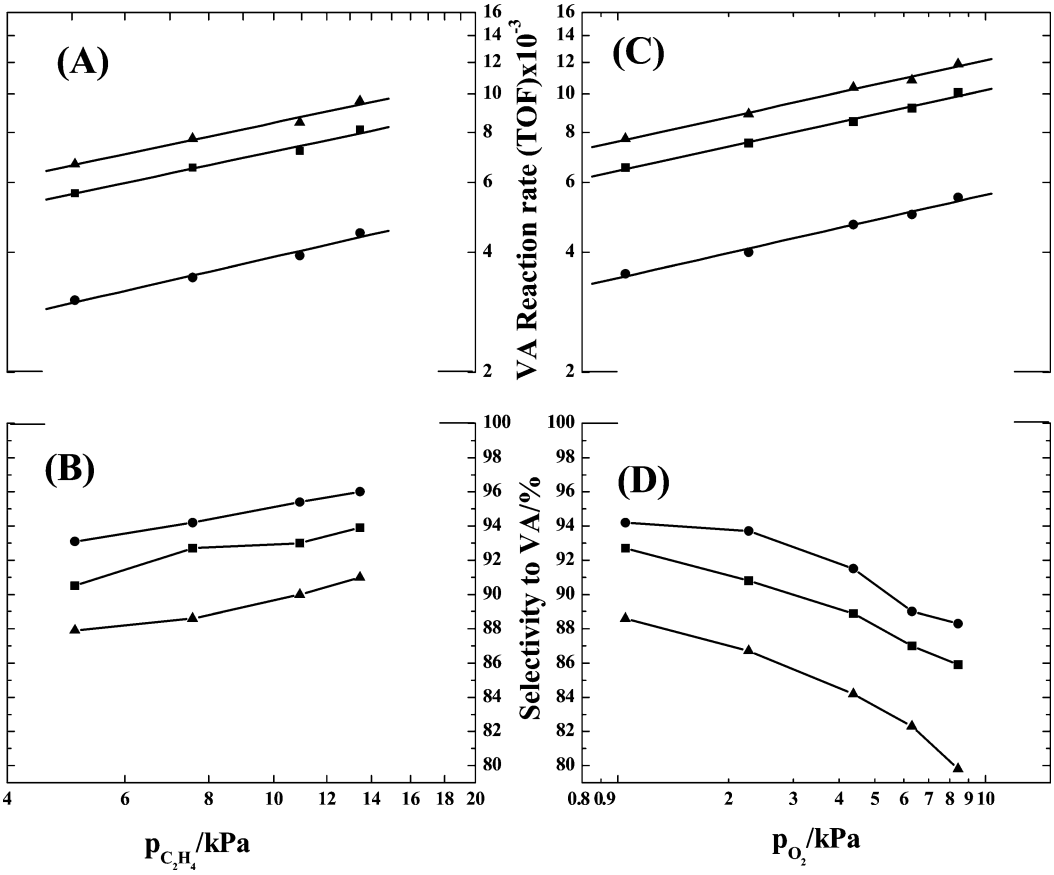

Fig. 4. $p_{C_2H_4}$-dependent reaction rate for VA synthesis (A) and selectivity (C) at feed gas of $p_{C_2H_4} = 5.0$–14.0 kPa, $p_{O_2} = 1.0$ kPa, $p_{AcOH} = 2.0$ kPa, the remainder N_2; p_{O_2} = dependent reaction rate for VA synthesis (B) and selectivity (D) at feed gas of $p_{C_2H_4} = 7.5$ kPa, $p_{O_2} = 1.0$–8.4 kPa, $p_{AcOH} = 2.0$ kPa, remainder N_2. Reaction conditions: 0.1–1.0 g of the Pd–Au catalyst, 30–60 ml/min of flow rate, temperatures of 433 (▲), 413 (■), and 393 K (●).

3.2. Kinetics of VA synthesis

The formation of VA as a function of partial pressure of oxygen (p_{O_2}) and ethylene ($p_{C_2H_4}$) at 393, 413, and 433 K is displayed in Fig. 4. As shown in Fig. 4A, with an increase in $p_{C_2H_4}$ the reaction rate increases from 5.0 to 14.0 kPa, for p_{O_2} kept constant at 1.0 kPa, yielding reaction orders of 0.38, 0.35, and 0.35 at 393, 413, and 433 K, respectively. At the same time, the rate of VA production increased by a factor of 2 with an increase in the temperature from 393 to 413 K, whereas only a 25% increase was found with an increase from 413 to 433 K. Meanwhile, the variation in selectivity shows the same trend with varying $p_{C_2H_4}$, as shown in Fig. 4B. At 393 K, the selectivity increased from 93.0 to 96.0% when $p_{C_2H_4}$ was increased from 5.0 to 14.0 kPa. However, the selectivity was significantly reduced with an increase in the temperature. For example, at $p_{C_2H_4} = 5.0$ kPa, the selectivity dropped from 93.0 to 88.0% with an increase in the temperature from 393 to 433 K. Enhancement of ethylene combustion with an increase in the temperature is presumed to be responsible for the loss of selectivity; this issue is discussed later in the text.

We measured the influence of p_{O_2} on the rate of VA production similarly by maintaining $p_{C_2H_4}$ at 7.5 kPa (see Fig. 4C): orders of 0.20, 0.20, and 0.21 were measured accordingly at 393, 413, and 433 K, respectively. However, in contrast to the results of Fig. 4B, a dramatic decrease in selectivity was observed with an increase in p_{O_2} (see Fig. 4D). At 393 K, the selectivity decreased from 94.0 to 89.0% with an increase in p_{O_2} from 1.0 to 8.4 kPa.

Reaction rates are shown in Fig. 5 as a function of temperature. For $p_{C_2H_4}$ fixed at 7.5 kPa and p_{O_2} varying from 1.0 to 8.4 kPa, the VA rates varied significantly with temperature. Temperature effects can be roughly classified into two regions: I, 393–413 K, and II, 413–433 K. The rates in Region I increase faster with temperature compared with the corresponding rates in Region II, suggesting that ethylene combustion is favored at temperatures greater than 413 K. Apparent activation energies (E_a) of 40.0 ± 4.0 kJ/mol for Region I (very close to the E_a's of 39.0 kJ/mol measured for Pd-only catalysts) and 15.0 ± 4.0 kJ/mol for Region II follow from the Arrhenius data.

The kinetics of VA synthesis for the Pd-only catalyst has also been measured under identical conditions (for more details, see Ref. [9]). A comparison of the kinetic parameters for the two catalysts is displayed in Table 1. Table 1 shows that the difference between the two catalysts is principally the reaction order with respect to C_2H_4, that is, negative

Table 1
Kinetic parameters for the synthesis of VA over Pd–Au and Pd catalysts, power law functionality: $r_{VA} = kp_{C_2H_4}^{\alpha} p_{O_2}^{\beta}$

Catalyst	T (K)	Constant rate (k) $\times 10^{-2}$ s^{-1}	α	β	γ_{VA}[a] $\times 10^{-3}$ s^{-1}
Pd–Au	393	2.45	0.38 ± 0.04	0.20 ± 0.02	3.48
Pd–Au	413	4.03	0.35 ± 0.01	0.20 ± 0.03	6.47
Pd–Au	433	4.70	0.35 ± 0.03	0.21 ± 0.03	7.54
Pd-1	413	0.03	-0.34 ± 0.02	0.18 ± 0.01	0.21

[a] Rates obtained with $p_{C_2H_4} = 5.0$ kPa, $p_{O_2} = 1.0$ kPa, $p_{AcOH} = 2.0$ kPa, the remainder N_2. Turnover frequency (TOF) was calculated based on: $r_{TOF,VA} = r_{VA} m_{Pd}/D$, m_{Pd} = Pd atom weight, D = dispersion of Pd. The dispersion of Pd was estimated from the Pd particle size measured by TEM; ca. 40% dispersion of Pd was estimated for the Pd–Au/SiO_2 catalyst, corresponding to ca. 3.2 nm Pd–Au particles.

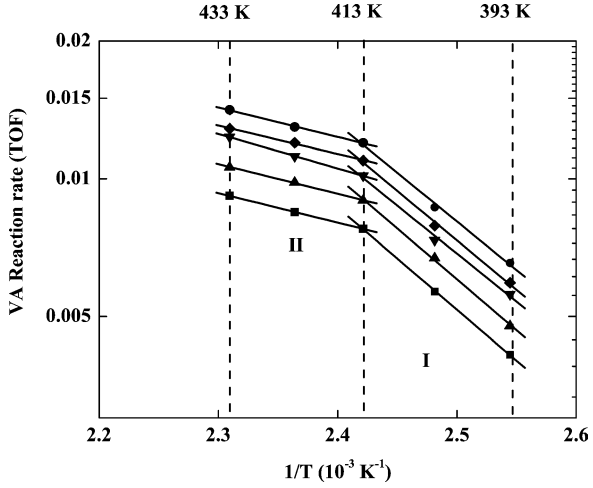

Fig. 5. Arrhenius plots for VA synthesis on the Pd–Au catalysts. Region I: 393–413 K, II: 413–433 K. Same reaction conditions as in Fig. 3; varying p_{O_2} at 1.0 (■), 2.2 (▲), 4.2 (▼), 6.3 (◆), and 8.4 (●), while keeping $p_{C_2H_4} = 7.5$ kPa, $p_{AcOH} = 2.0$ kPa, remainder N_2.

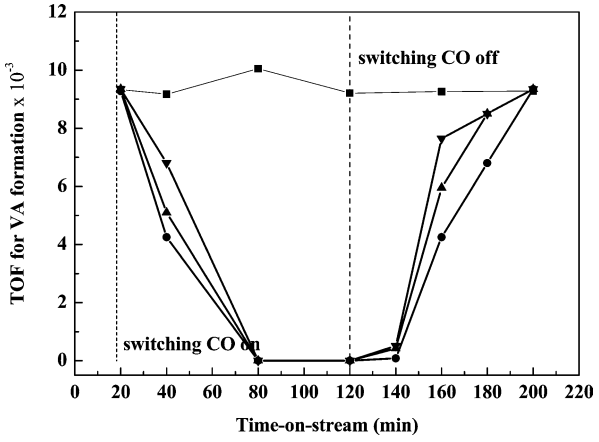

Fig. 6. VA synthesis in the presence of CO at 413 K in the feed gas of $p_{C_2H_4} = 7.5$ kPa, $p_{O_2} = 1.0$ kPa, $p_{AcOH} = 2.0$ kPa, remainder N_2, p_{CO}: 0 (■), 0.1 (▼), 0.5 (▲), and 1.0 (●).

for the Pd-only catalyst and positive for the Pd–Au catalyst, whereas the rate of VA production is significantly improved by alloying Pd with Au. It is worth noting that the reaction order with respect to acetic acid is approximately zero for both catalysts; therefore the effects of acetic acid were not explored further.

3.3. VA synthesis in the presence of CO

The influence of CO on VA formation was investigated with the use of a mixture of C_2H_4 (7.5 kPa), O_2 (1.0 kPa), CO (0–1.0 kPa), and AcOH (2.0 kPa) at 413 K over the Pd–Au catalyst. Fig. 6 shows that the addition of CO strongly poisons the active sites and suppresses VA formation. Interestingly, the reaction time (ca. 60 min) for full inhibition of reactivity upon the introduction of CO is equal to the restoration time required after elimination of CO, independent of the CO partial pressure. Furthermore, it is worth noting that the CO_2 concentration decreased simultaneously with the decline in the rate of VA formation. In addition, the onset of CO oxidation over the same catalyst was detected at 483 K (2.0% conversion with a feed gas of 3.0% CO and 3.0% O_2). Therefore, it can be excluded that O_{ads}, essential for VA synthesis, is consumed by the CO oxidation reaction. Analogous results were observed for the Pd-only catalyst (results not shown for the sake of brevity).

3.4. Kinetics of CO oxidation

CO oxidation kinetics was investigated over the same catalysts as used for VA synthesis. The kinetic parameters and their comparison with data from the literature, including the kinetics over supported Pd and single-crystal Pd catalysts, are listed in Table 2. It can be seen that a negative reaction order for CO (α_{CO}) and a positive order for O_2 (α_{O_2}) were observed for both catalysts, in agreement with previous studies; however, the absolute value of the CO order ($|\alpha_{CO}|$) for the Pd–Au catalyst is lower than that for the Pd-only catalyst.

3.5. CO-TPD and C_2D_4-TPD on thick Pd and Pd–Au films

To avoid CO disproportionation in the TPD measurements, a phenomenon previously reported for CO desorption over supported Pd particles or technical Pd/support catalysts [31,32], TPD of CO and C_2D_4 was carried out over Pd (> 10 layers) and Pd–Au alloy (atom ratio of 1:1 of Pd/Au) films in UHV. It was noted that VA synthesis had already been carried out on a well-defined Pd(100) surface, and the results were found to closely match those observed

Table 2
Kinetic parameters for CO oxidation over Pd–Au and Pd catalysts, power law functionality: $r_{VA} = k p_{CO}^{\alpha} p_{O_2}^{\beta}$

Catalyst	Conditions	α	β	Reference
Pd(100)	500 K, p_{CO}/p_{O_2}: 0.07–0.7 kPa	-1.2 ± 0.1	1.2 ± 0.1	[22]
Pd(111)	500 K, p_{CO}/p_{O_2}: 0.07–0.7 kPa	–	0.97 ± 0.1	[23]
5% Pd/SiO_2	<383 K, p_{CO}/p_{O_2}: 0.1–10.0 kPa	-0.8 ± 0.2	0.8 ± 0.2	[30]
Pd–Au	483 K, p_{CO}/p_{O_2}: 3.0–10.0 kPa	-0.35 ± 0.02	0.57 ± 0.03	This study
Pd-1	553 K, p_{CO}/p_{O_2}: 3.0–2.0 kPa	-1.0 ± 0.1	0.81 ± 0.1	This study

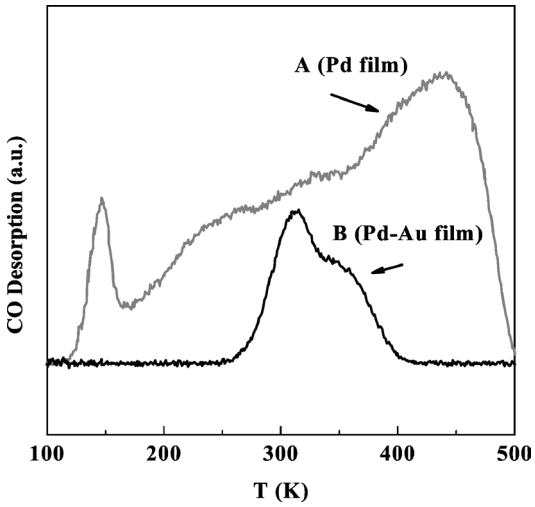

Fig. 7. CO-TPD spectra for thick Pd film (A) and Pd–Au alloy film (B), ramp rate = 5 k/s.

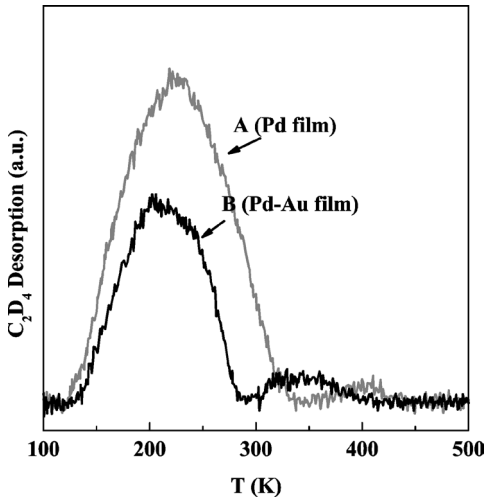

Fig. 8. C_2D_4-TPD spectra for thick Pd (A) and Pd–Au films (B), ramp rate = 5 k/s.

under realistic reaction conditions over supported Pd catalysts [33]. Therefore, we assume that the structure of the active sites on a Pd film should be similar to that of supported, high-area catalysts. For CO-TPD from multilayer Pd (Fig. 7A), two distinct features appear at 150 and 430 K, with multiple features apparent between these two. These features closely resemble those observed for Pd(111) [29]. By analogy, we assume that the feature at 150 K corresponds to desorption of CO from a-top/hollow sites, and that at 430 K, to bridging sites. The appearance of a feature at 430 K is in excellent agreement with previous results for CO desorption from thick Pd films ($\theta_{Pd} \geqslant 20$, at 499 K [34]), bulk Pd(111)/Mo(111) (at 480 K [35]), and Pd/α-Al_2O_3 (at 475 K [36]). In a comparison of peak areas, the Pd film surface exhibits a high density of bridging sites, consistent with IR data for adsorbed CO. In contrast, the CO-desorption feature for the Pd film upon alloying with Au is substantially modified. A TPD from the Pd–Au film shows a prominent desorption feature at 300 K with a shoulder at 350 K (see Fig. 7B); it is worth noting that the capacity of the alloy surface for CO is only one-third that of the Pd film as deduced from the TPD peak areas.

TPD data were also collected for the Pd film after adsorption of deuterium-substituted ethylene, C_2D_4. Fig. 8A shows that ethylene desorbs from the Pd film between 120 and 350 K, with a distinct desorption maximum at ca. 225 K and a small secondary feature at 400 K. A similar desorption profile was also observed for the Pd–Au alloy film; however, the two features shift to 200 and 350 K, respectively, and the quantity of C_2D_4 desorbed is $\sim$30% less compared with the Pd films (see Fig. 8B). Similar experiments for a $Pd/Al_2O_3/NiAl(110)$ model catalyst [37] show a prominent feature below 230 K in the C_2D_4-TPD spectra for small Pd particles. In contrast, a single desorption peak near 300 K was observed for the single-crystal surfaces [38–40].

4. Discussion

4.1. Reaction rate and selectivity for VA synthesis

The kinetic data for VA synthesis over Pd-based catalysts are consistent with the reaction proceeding via a Langmuir–Hinshelwood mechanism. For VA synthesis over the Pd–Au catalyst, as depicted in Figs. 4A and 4B, a $p_{C_2H_4}$-dependent rate increase was observed at temperatures of 393, 413, and 433 K, consistent with a coverage of C_2H_4-derived species less than saturation on the Pd–Au surface. This contrasts with the behavior observed for the Pd-only catalyst, where the coverage of C_2H_4 was estimated to be at saturation based on the negative order of the rate with respect to $p_{C_2H_4}$ at similar reaction conditions [9]. On the other hand, a positive reaction order with respect to p_{O_2} for both catalysts suggests that O_2 adsorption is blocked by adsorbed C_2H_4, consistent with O_2 being the rate-limiting reagent on the Pd-only cat-

alyst (this point has been discussed in detail previously in Ref. [9]). Moreover, the reaction orders at all three temperatures approximate those for the Pd–Au catalyst, consistent with a single reaction mechanism being operative in VA synthesis, independent of the reaction conditions.

As illustrated in Figs. 4C and 4D, the selectivity for VA formation increases with an increase in $p_{C_2H_4}$ and decreases with an increase in p_{O_2}. Two competitive reactions are operative for VA synthesis over supported Pd-only catalysts [5,6,28]: ethylene combustion and VA synthesis. For a 5 wt% Pd/SiO_2 catalyst, a mechanistic study of ethylene combustion in either a VA reactant mixture or an acetic acid-free gas mixture shows limited dissociative adsorption of oxygen, deduced from the negative order of the reaction with respect to $p_{C_2H_4}$ [28]. For a Pd–Au catalyst, the rise in selectivity with an increase in $p_{C_2H_4}$ may be due to an increase in the C_2H_4 coverage, which favors VA synthesis over ethylene combustion. That is, the coverage of C_2H_4 on the Pd–Au catalyst is far from saturation. The decrease in selectivity that occur with the rise in p_{O_2} illustrates that an excess of adsorbed oxygen (O_{ad}) accelerates ethylene combustion more so than VA formation. Therefore, to achieve a high selectivity for VA formation, a high $p_{C_2H_4}/p_{O_2}$ ratio is essential.

VA formation and combustion are greatly influenced by the reaction temperature. As shown in Fig. 5, two Arrhenius regions are apparent within the temperature range of 393–433 K. Over a wide range of p_{O_2} with a fixed $p_{C_2H_4}$, the temperature-dependent rate increases more significantly between 393 and 413 K (Region I) than between 413 and 433 K (Region II), indicating that ethylene combustion was significantly enhanced at elevated temperatures, depletes O_{ad}, and suppresses the formation of VA. A possible consequence may be the reduction of the C_2H_4 coverage as the temperature is increased. On the other hand, a larger fraction of C_2H_4 is likely dissociated to a hydrocarbonaceous residue with an increase in the temperature; this species, in turn, is more easily converted by oxygen to CO_2. Consequently, the selectivity is dramatically reduced with an increase in temperature, as shown in Figs. 4B and 4D.

Interestingly, the similarity of the E_a values for the two catalysts (Region I for Pd–Au) suggests that VA synthesis mainly occurs at Pd sites.

4.2. Structure modification from Pd to Pd–Au

The modification of Pd catalysts with Au has been extensively investigated [10–19]. Au has been found to preferentially segregate to the surface in Pd–Au alloys [19,41]; however, a more recent study showed that Pd–Au clusters consist of a Au-rich core covered with a monolayer of Pd [12]. EDS analysis showed Au enrichment on a reduced Pd–Au surface. Further Au enrichment was detected for the reacted catalyst, because of the alloying of Pd and Au as indicated by XRD in a similar potassium-doped catalyst [42]. Au is thought to modify Pd by either an electronic or a geometric effect.

Roudgar et al. [43], who used a Pd–Au film, argued that geometric effects are more important than electronic effects in the modification of Pd–Au reactivity. For a Pd(111)/Au model Baddeley et al. [44] also suggested that the formation of Pd_6Au and Pd_7 surface ensembles, rather than an electronic perturbation of Pd by Au, plays an essential role in the improvement of reactivity. Alternatively, Gleich et al. [45] found that $PdAu_6$ ensembles were formed on a Au/Pd(111) surface, in the presence of isolated Pd atoms in a Au matrix. As a result, the adsorption sites were remarkably reduced on a Pd–Au alloy surface in comparison with a Pd-only surface. Several CO-desorption experiments have shown that CO coverage decreases with an increase in the amount of Au in a Pd–Au alloy [44–47]. Accordingly, we attribute the pronounced drop in the amount of CO and C_2D_4 adsorbed on a Pd–Au alloy compared with a Pd-only surface to reduction of Pd adsorption sites. CO-TPD (Fig. 7) showed that the adsorption sites with strong (feature at 430 K) and weak (feature at 150 K) binding energies on Pd vanished upon alloying with Au and were replaced with adsorption sites of moderate binding energy on the Pd–Au surface. Correspondingly, the reduction in the density of Pd–Pd ensembles on the Pd–Au surface is also responsible for the decrease in C_2D_4 adsorption amount and binding energy (downshift of the desorption peak), as depicted in Fig. 8. Interestingly, the addition of Au to Pd also decreased the binding energy of oxygen binding to the surface and reduced the oxygen coverage [15,46].

4.3. Kinetics and mechanism

As mentioned above, the addition of Au to Pd alters the Pd ensembles and modifies the binding energy of related adsorption sites. It was shown that only those sites with moderate bonding energy remain and are crucial to the catalytic reaction. It is reasonable that the modification of the surface Pd atom configuration in the Pd–Au catalyst is a key to the change of kinetics for VA synthesis and CO oxidation, as shown in Tables 1 and 2.

Before we analyze the kinetics, it is worth reviewing the effects of CO on VA synthesis. Fig. 6 shows that VA synthesis on the Pd–Au catalyst is poisoned reversibly by the adsorption of CO on the Pd–Au catalyst over a wide range of CO concentrations. This suggests that the two reactions share the same active sites and that adsorbed CO on the Pd–Au surface blocks the adsorption and/or migration of either C_2H_4 or O_2. For the Pd-only catalyst, the negative reaction order with respect to C_2H_4/CO and the positive reaction order with respect to O_2 indicate that both reactions proceed via a Langmuir–Hinshelwood mechanism within the low reaction rate region, where dissociative adsorption of O_2 is the rate-determining step. This behavior has been shown for CO oxidation from Pd single crystal in the UHV system [22,23] to high-surface-area supported Pd catalysts [30]. For the Pd–Au catalyst, however, the reaction order with respect to C_2H_4 changes to a positive value for VA synthesis; the or-

der for CO in CO oxidation is still negative, yet much less so; the orders for O_2, however, for both reactions are positive. Hence, we infer that the dissociative adsorption of O_2 is unlikely to be the rate-determining step in VA synthesis on the Pd–Au surface because of a less than saturating coverage of C_2H_4 on the Pd–Au surface. This lack of saturation may enhance oxygen adsorption or mobility in spite of a significant reduction in the amount of O_2 adsorbed that occurs as we go from Pd to Pd–Au [15]. For the Pd–Au catalyst, CO oxidation exhibits quite different kinetics compared with VA synthesis, perhaps because of a variation in the binding energy of CO and C_2H_4.

In addition, a temperature-screening experiment for CO oxidation (3% CO and 3% O_2, 30 mg catalyst; not shown for the sake of brevity) revealed that the onset temperature for CO oxidation shifted from 553 K for the Pd-only catalyst to 483 K for the Pd–Au catalyst. Moreover, CO oxidation is purported to occur exclusively on Pd in a Pd-rich alloy surface, since Au/SiO_2 shows no reactivity [47]. In a study of electrochemical oxidation of CO, Gossner et al. [48] suggested that the high rate on Pd–Au alloy may be ascribed to the migration of O_{ad} from Pd to Au, which presumably would enhance O_2 adsorption. The key reaction steps are

$$\mathrm{Pd} + \mathrm{CO} \rightarrow \mathrm{Pd\text{–}CO}, \tag{2}$$

$$\mathrm{Pd} + \mathrm{O} \rightarrow \mathrm{Pd\text{–}O}, \tag{3}$$

$$\mathrm{Pd\text{–}O} + \mathrm{Au} \rightarrow \mathrm{Pd} + \mathrm{Au\text{–}O}, \tag{4}$$

$$\mathrm{Pd\text{–}O} + \mathrm{Pd\text{–}CO} \rightarrow 2\mathrm{Pd} + \mathrm{CO_2}, \tag{5}$$

$$\mathrm{Au\text{–}O} + \mathrm{Pd\text{–}CO} \rightarrow \mathrm{Au} + \mathrm{Pd} + \mathrm{CO_2}. \tag{6}$$

A key remaining question is whether the migration of O_{ad} to Au occurs on the Pd–Au surface in VA synthesis and whether this migration plays a critical role in improving the reactivity and selectivity.

5. Conclusions

1. High-surface-area SiO_2-supported Pd and Pd–Au alloy catalysts were prepared. XRD and TEM-EDS show that the Pd–Au alloy particles are highly dispersed and enriched at the surface with Au.

2. CO/C_2D_4-TPD experiments on films of Pd and Pd–Au show a remarkable drop in the amount of CO and C_2H_4 adsorbed, suggesting that critical Pd adsorption sites are significantly reduced upon alloying with Au. Pd ensembles, such as $PdAu_6$ or $PdAu_5$, are likely created on the Pd–Au surface and are responsible for the subsequent change in the reaction mechanism.

3. Comparative kinetics of VA synthesis and CO oxidation on Pd-only and Pd–Au catalysts is consistent with both reactions proceeding via a Langmuir–Hinshelwood mechanism. For the Pd-only catalyst, the negative order with respect to C_2H_4/CO and positive order with respect to O_2 are consistent with dissociative adsorption of oxygen being the rate-determining step and the inhibition of oxygen adsorption by C_2H_4 and/or CO. For the Pd–Au catalyst, the reaction order with respect to C_2H_4 is positive. The adsorption data suggest that the change in the reaction mechanism for the Pd–Au catalyst relates to the decrease in the C_2H_4/CO coverage and to the increase in surface capacity for oxygen. This increase in oxygen coverage is responsible for the increase in reactivity in the Pd–Au catalyst.

Acknowledgments

We acknowledge with pleasure the support of this work by the Department of Energy, Office of Basic Energy Sciences, Division of Chemical Sciences, and the Robert A. Welch Foundation. We also thank Dr. Les Wade of the Celanese Chemical Company for helpful discussions throughout the course of this work.

References

[1] I.I. Moiseev, M.N. Vargaftik, Y.K. Syrkin, Dokl. Akad. SSSR 133 (1960) 377.
[2] B.T. Charles, US Patent 4,048,096 (1977).
[3] M. Nakamura, Y. Fujiwara, T. Yasui, US Patent 4,087,622 (1978).
[4] K. Sennewald, H. Glaser, US Patent 3,761,513 (1973).
[5] B. Samanos, P. Boutry, R. Montarnal, J. Catal. 23 (1971) 19.
[6] S. Nakamura, T. Yasui, J. Catal. 17 (1970) 366.
[7] S. Nakamura, T. Yasui, J. Catal. 23 (1971) 315.
[8] A.H. Zaidi, Appl. Catal. 30 (1987) 131.
[9] Y.-F. Han, D. Kumar, D.W. Goodman, J. Catal. 230 (2005) 362.
[10] M. Neurock, J. Catal. 216 (2003) 73.
[11] M. Neurock, D. Mei, Top. Catal. 20 (2002) 5.
[12] S.N. Reifsnyder, H.H. Lamb, J. Phys. Chem. B 103 (1999) 321.
[13] C.J. Baddeley, M. Tikhor, C. Hardacre, J.R. Lomas, R.M. Lambert, J. Phys. Chem. 100 (1996) 2189.
[14] A.M. Venezia, V. La Parola, G. Deganello, B. Pawelec, J.L.G. Fierro, J. Catal. 215 (2003) 317.
[15] D.L. Weissman-Wenocur, W.E. Spicer, Surf. Sci. 133 (1983) 499.
[16] D.L. Weissman-Wenocur, P.M. Stefan, B.B. Pate, M.L. Shek, L. Lindau, W.E. Spicer, Phys. Rev. B 27 (1983) 3308.
[17] X.Y. Shen, D.J. Frankel, G.J. Lapeyre, R.J. Smith, Phys. Rev. B 33 (1986) 5372.
[18] L. Hilaire, P. Legare, Y. Holl, G. Maire, Surf. Sci. 103 (1981) 125.
[19] S. Jablonsk, H. Overbury, G.A. Somorjai, Surf. Sci. 65 (1977) 578.
[20] T. Dellwig, J. Hartmann, J. Libuda, I. Meusel, G. Rupprechter, H. Unterhalt, H.-J. Freund, J. Mol. Catal. A: Chem. 162 (2000) 51.
[21] M.P. Harold, M.E. Garske, J. Catal. 127 (1991) 553.
[22] J. Szanyi, W.K. Kuhn, D.W. Goodman, J. Phys. Chem. 98 (1994) 2972.
[23] J. Szanyi, W.K. Kuhn, D.W. Goodman, J. Phys. Chem. 98 (1994) 2978.
[24] M. Hirsimaki, P. Nieminen, M. Valden, Surf. Sci. 482 (2001) 147.
[25] A. Martínez-Arias, B. Hungría, M. Fernández-García, A. Iglesias-Juez, J.A. Anderson, J.C. Conesa, J. Catal. 221 (2004) 85.
[26] A. Guerrero-Ruiz, S.W. Yang, Q. Xin, A. Maroto-Valiente, M. Benito-Gonzalez, I. Rodriguez-Ramos, Langmuir 16 (2000) 8100.
[27] X. Xu, J. Szanyi, Q. Xu, D.W. Goodman, Catal. Today 21 (1994) 57.
[28] Y.-F. Han, D. Kumar, C. Sivadinarayana, D.W. Goodman, J. Catal. 224 (2004) 60.
[29] W.K. Kuhn, J. Szanyi, D.W. Goodman, Surf. Sci. 274 (1992) L611.
[30] N.W. Cant, P.C. Hicks, B.S. Lennon, J. Catal. 54 (1978) 372.
[31] V. Matolin, E. Gillet, Surf. Sci. 238 (1990) 75.

[32] M.A.S. Baldanza, L.F. de Mello, A. Vannice, F.B. Noronha, M. Schmal, J. Catal. 192 (2000) 64.
[33] D. Kumar, Y.-F. Han, D.W. Goodman, unpublished.
[34] J.M. Heitzinger, S.C. Gebhard, B.E. Koel, Surf. Sci. 275 (1992) 209.
[35] C. Xu, D.W. Goodman, Surf. Sci. 360 (1996) 249.
[36] V. Matolin, V. Johánek, I. Stará, N. Tsud, K. Veltruská, J. Electron Spectrosc. Relat. Phenom. 114–116 (2001) 327.
[37] Sh. Shaikhutdinov, M. Heemeier, M. Bäumer, T. Lear, D. Lennon, R.J. Oldman, S.D. Jackson, H.-J. Freund, J. Catal. 200 (2001) 330.
[38] E.M. Stuve, R.J. Madix, C.R. Brundle, Surf. Sci. 152/153 (1985) 532.
[39] W.T. Tysoe, G.L. Nyberg, R.M. Lambert, J. Phys. Chem. 88 (1984) 1960.
[40] T. Sekitani, T. Takaoka, M. Fujisawa, M. Nishijima, J. Phys. Chem. 96 (1992) 8462.
[41] G. Maire, L. Hilaire, P. Legare, F.G. Gault, A. O'Cinneide, J. Catal. 44 (1976) 293.
[42] Y.-F. Han, D. Kumar, C. Sivadinarayana, D.W. Goodman, Catal. Lett. 94 (2004) 131.
[43] A. Roudgar, A. Groß, Phys. Rev. B 67 (2003) 033409.
[44] C.J. Baddeley, R.M. Ormerod, A.W. Stephenson, R.M. Lambert, J. Phys. Chem. 99 (1995) 5146.
[45] B. Gleich, M. Ruff, R.J. Behm, Surf. Sci. 386 (1997) 48.
[46] D.D. Eley, P.B. Moore, Surf. Sci. 111 (1981) 325.
[47] A.M. Venezia, L.F. Liotta, G. Pantaleo, V. La Parola, G. Deganello, A. Beck, Zs. Koppány, K. Frey, D. Horváth, L. Guczi, Appl. Catal. A: Gen. 21 (2003) 359.
[48] K. Gossner, E. Mizera, J. Electroanal. Chem. 98 (1979) 37.